Antenna Structures: Evaluation of Field Measurements of Reflector Distortions

B. Marcus and M. S. Katow
DSIF Engineering Section

Field measurements of reflector distortions, using the theodolite angle differences and fixed arc lengths from the vertex of the paraboloid, are based on apparent displacements normal to the line of sight. Two computing methods are described which use directions information from the structural computer analysis to upgrade the readings in the pathlength errors sense. Comparative rms values of the 1/2 pathlength errors, after a paraboloid best fit, resulting from the field measurements, the analytical analysis, and the rms equivalences to RF radio star measurements, are overlayed on an rms surface tolerance versus elevation angle chart for the 64-m-diam antenna. Close rms agreements allow designation of an error tolerance of ±0.08 mm (0.003 in.) for the field-measured rms values.

I. Introduction

The state-of-the-art method of measuring distortions of a large ground-based antenna uses an angle-measuring theodolite mounted on the axis of symmetry just above the vertex of the paraboloid. The only other dimension measured is the arc length from the vertex to the target located on the surface of the paraboloid (Fig. 1). Since the theodolite can only measure apparent deflections measured normal to its line of sight, the actual RF pathlength error may not be evaluated within useful precision when the Z components of the readings are input to the rms computer program (Ref. 1). This anomaly was apparent since the first output of the three vector components from the analytical solutions.

One solution proposed by R. Levy (Ref. 2) uses analytically computed three-component distortions read by simulated field readings by the theodolite method. The difference in the two rms values can then be applied as corrections to the field-measurement values. This method, revised to use vector analysis, is described and is now incorporated as subroutine ANAFLD as part of the rms package (Type D).

Another solution method, also described in this article, combines the single-dimension field measurement with direction vectors from the analytic solution to determine the correct rms value. Subroutine FIELD modifies the data before its input to the best fitting computation (Type C).

Table 1 defines terms used in the discussion that follows.

II. Process of Field Measurement

Normally, the surface panels are first installed and adjusted close to the center of the adjustment range with the edges faired from one panel to the next one at zenith look. Then, the target mounting holes are drilled to predetermined arc distances from the vertex of the paraboloid using a strap gage. The change in arc distances is assumed presently to be negligible for the different elevation angle positions.

At an elevation angle selected for the "perfect" paraboloid position (45-deg for the 64-m-diam antenna), each

Table 1. Definition of terms

Deflection vector	vector from the original position of the target point to its deflected position
Field reading **QT**	the projection of the deflection vector onto the line which passes through the target point and is perpendicular to the line of sight. The unit vector in the direction $\mathbf{QT}/\|\mathbf{QT}\|$ has components, denoted F_X, F_Y, F_Z. Explicitly: if the target point Q has coordinates X, Y, Z, then $$F_X = \frac{-X \sin\psi}{(X^2+Y^2)^{1/2}}, \quad F_Y = \frac{-Y \sin\psi}{(X^2+Y^2)^{1/2}},$$ $$F_Z = \cos\psi$$
Instrument angle reading ψ	the angle between the line of sight and its projection onto the zero-plane
Line-of-sight vector	vector from the point (0,0,38 cm) (0,0,15 in.) to the target point
Measuring-plane	plane determined by the Z-axis and the line of sight; field measurements are made in this plane
X-axis	line in XY-plane perpendicular to Y-axis; this line is parallel to the elevation axis of an az–el antenna
XY-plane	plane perpendicular to Z-axis, passing through the vertex
Y-axis	line which passes through the paraboloid vertex and points to zenith when elevation angle is 0 deg (to horizon)
Z-axis	axis of symmetry of undeflected paraboloid
Zero-plane	plane perpendicular to Z-axis, passing through the theodolite rotation axes and the datum targets; this is the reference plane for theodolite measurements

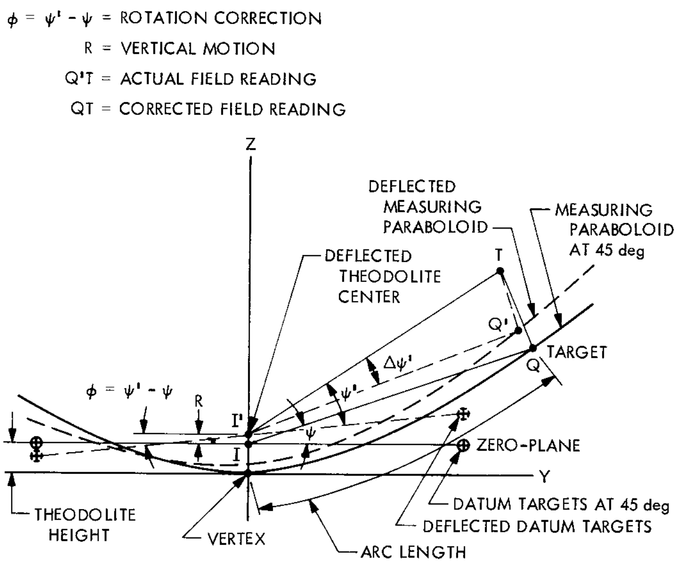

Fig. 1. Field measurement scheme

target is sighted with a theodolite located above the vertex and on the axis of symmetry, with the zero-plane aligned to the four datum reference targets located in the reflector structure. Two of the datum targets are located just above the elevation bearings along the X-axis and the other two are in the wheel girder of the 64-m-diam antenna reflector structure along the Y-axis. The angle ψ between the target and the zero-plane, calculated from the focal length and arc distances of the paraboloid, is used to set the targets of the panels for the "perfect" paraboloid case (Fig. 1).

After the reflector is rotated to another elevation angle, the reading process is repeated for the same target points. There will be a change in the theodolite's angle ψ, denoted as ψ' in Fig. 1. Thus, the apparent deflection of target Q will be a vector **Q′T**, which is normal to the line of sight.

III. Correction to Field Measurement from Motion of the Measuring Paraboloid (Type C)

Due to the change in direction of the gravity load for the different elevation angle positions, the datum targets themselves deflect in a manner (Fig. 1) which effectively:

(1) Rotates the measuring paraboloid as determined by the datum plane about the X-axis by angle ϕ. Since ϕ is very small, we can make the approximation: $\phi \sim \sin\phi$.

(2) Offsets the datum plane in the direction of the symmetry axis (Z-axis) by offset **R**.

It can thus be concluded that the field measurements, at elevation angles other than the perfect paraboloid angle, are made with respect to a rotated and translated coordinate system. Therefore, correction factors to **Q′T** must be applied to obtain the true field readings (**QT**) as follows:

$$\mathbf{QT} = \mathbf{Q'T} + \mathbf{CO} + \mathbf{CR}$$

where the vector which represents the offset motion,

$$\mathbf{CO} = (0, 0, \mathbf{R}) \cdot \frac{\mathbf{QT}}{\|\mathbf{QT}\|}$$

$$= \mathbf{R} F_Z$$

$$= \mathbf{R} \cos\psi$$

and the vector which represents the rotation motion,

$$\mathbf{CR} = (0, -\phi Z, \phi Y)$$

$$= (0, -\phi Z, \phi Y) \cdot \frac{\mathbf{QT}}{\|\mathbf{QT}\|}$$

$$= -\phi Z F_Y + \phi Y F_Z$$

$$= \phi Y \left\{ \left[\frac{\sin\psi\,(X^2 + Y^2)^{1/2}}{4F} \right] + \cos\psi \right\}$$

since

$$Z = \frac{(X^2 + Y^2)}{4F}$$

IV. Correction of Field Measurements By Adding Direction Sense from Analytical Structural Analysis (Type C)

Figure 2 shows a typical analytically computed distortion vector **QP** with its three components **U**, **V**, and **W** in the X, Y, Z coordinate system.

When this vector is field read, the theodolite's field measuring plane $X'0Z$ rotates about the symmetric axis $0Z$ of the measuring paraboloid and picks up the change in angle ψ (Fig. 1) from point Q to P. Since the angle ψ measured by the theodolite to P and P' is essentially the same, the component **QP′** in the measuring plane is used in the calculations.

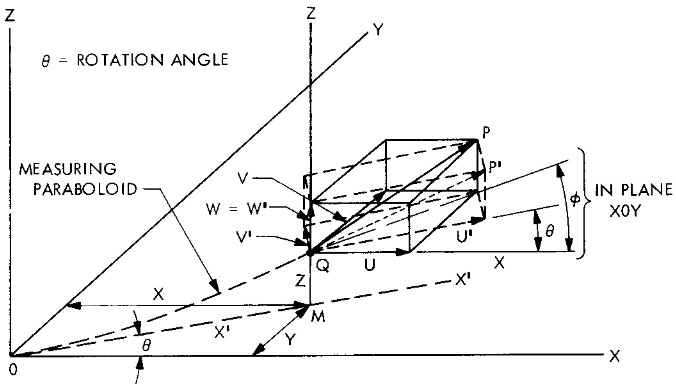

Fig. 2. Transformation of distortion vectors to measuring plane

To compute **QP′**, the distortion vector, **QP** in the X, Y, Z coordinate system must be transformed to the measuring plane $X'0Z$ (Appendix A). The resulting components are **U′**, **V′**, and **W**.

Since the magnitude of the distortion vector is very small with respect to distance X', the two lines of sight may be considered to be parallel for vector transformation calculations in the measuring plane. Of course, an optical micrometer used on the theodolite would conform exactly to the above assumption.

To upgrade the field-measured deflection **Q′T**, the direction sense from the analytically computed deflection vector **QP′** may be combined (Fig. 3). The direction sense of **QP′** determined by **U′** and **W** is combined with the magnitude and direction of the field measurement **QT** to determine the magnitude of the theoretically true deflection vector **QP′** (Appendix B).

The vector **QP′** is then normalized, that is, projected to the normal vector at point Q as **QN** since the magnitude of the normal error is a direct function of the pathlength error. A further conversion is made for compatibility to the rms analysis by dividing the normal by the tangent angle to result in a ΔZ deflection input (Appendix C).

There has arisen a problem connected with the accuracy tolerance of the field measurements when $\mathbf{QT} \cdot \mathbf{QP'}$ is near zero. This method requires more careful and accurate field readings at these target points. To eliminate the effect on the accuracy of the final rms number, any target reading for which $(\mathbf{QT} \cdot \mathbf{QP'}) < 0.05$ rad is presently deleted from the least squares analysis.

V. Computation of Theoretical Field Measurements from Analytically Computed Distortion Vectors (Type D)

The object of this computation is to simulate the theodolite method of measuring the analytically computed three-component distortion vectors. Then, the resulting rms output from the best-fit program may be compared to the rms output from field measurements without corrections.

As described in *Section IV* with Figs. 2 and 3, the field measurement vector **QT** subtends the "transposed to the measuring plane" vector **QP′**. However, now the magnitude as well as the direction of vector **QP′** are known. Therefore, vector **QT** may be computed and input to the best-fitting program to output the rms figure.

In order to satisfy the data requirements of the rms program coding, the ΔZ component **QK** of vector **QT** is used with **U** and **V** set equal to 0.

VI. Standard Field and Assumed Normal Direction Computations (Types A and B)

For computing the standard field measurement rms value (Type A), the ΔZ component **QK** of the apparent deflection vector **QT** normal to the line of sight is computed by dividing by the cosine of the instrument angle ψ (Fig. 4).

Instead of assuming that the deflection vector is normal to the line of sight, one can assume that all deflections are

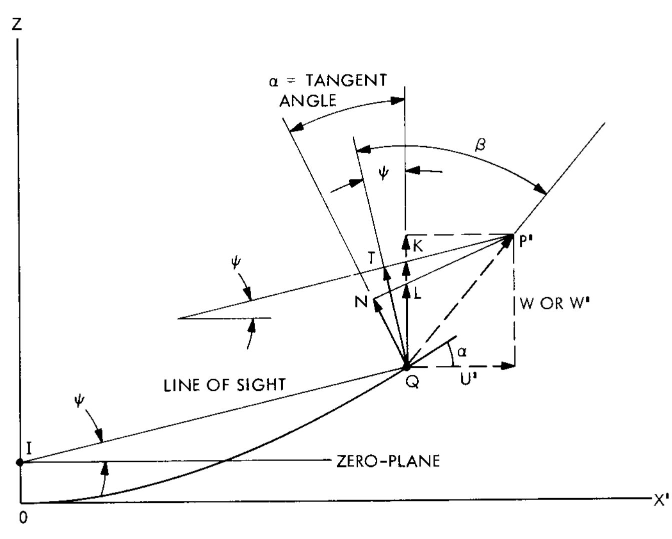

Fig. 3. Adding direction sense to field measurement

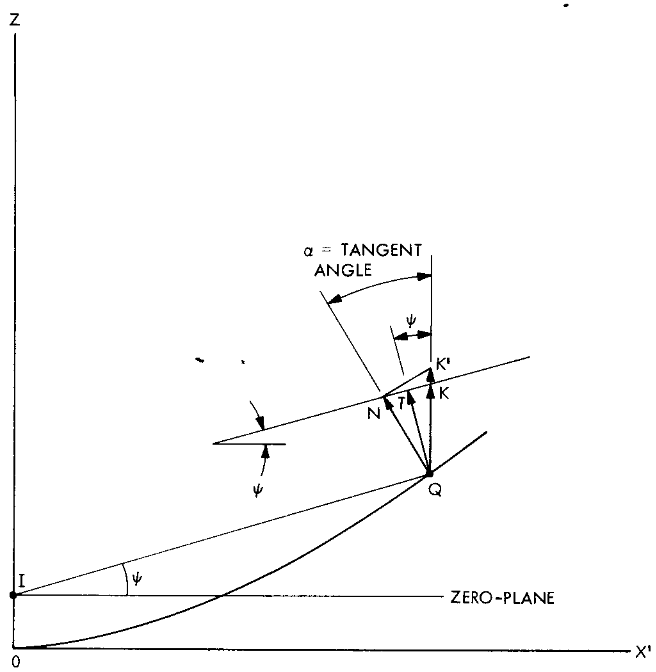

Fig. 4. Field measurement conversions for Type A or B analysis

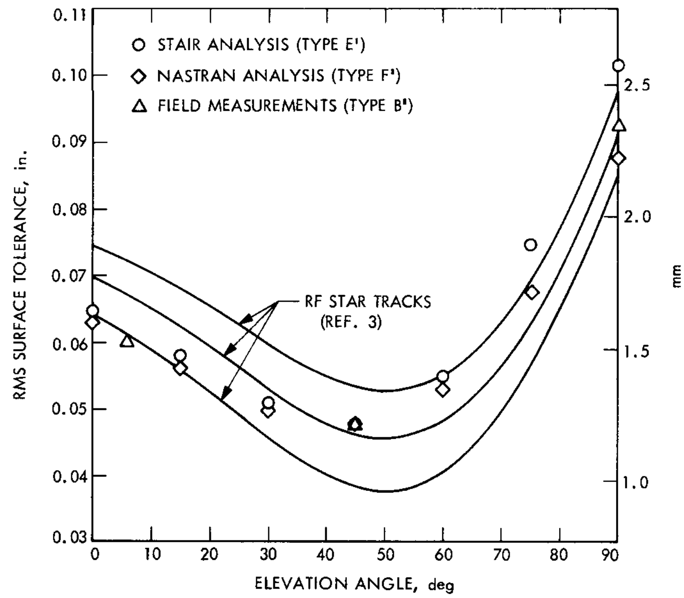

Fig. 5. RMS surface tolerance vs elevation angle (64-m-diam antenna, monocone cassegrain system; zenith attenuation = 0.06 dB)

in the line normal to the surface of the reflector (Type B). Using this assumption, **QN** equals **QT** divided by the cosine of $(\alpha - \psi)$ and it follows that **QK'**, the ΔZ component, is computed by dividing by the cosine of the tangent angle α. This results in the Type B rms answers.

VII. Results and Conclusions as Applied to the 64-m-diam Antenna Data

The different rms analysis methods for field measurements were typed from A to D and applied to the available 64-m-diam antenna data. Types E and F are from analytical computations. Since there was a large change (15,873 to 18,140 kg) (35,000 to 40,000 lb) in the weight of the cassegrain field cone assembly from the monocone to the tricone configuration, the systems were separately evaluated and the answers for reflector structure deflections exclusively are noted in Table 2.

At the present time, results from RF tests are available (Ref. 3) for only the monocone configuration; the answers projected from Table 2, with the addition of the surface panel rms distortions, etc., are overlayed on an upgraded curve from page 17 of Ref. 3 and reproduced here as Fig. 5. The upgrade of the curve is a change in the zenith attenuation from 0.036 to 0.060 dB.

The conclusions that can be made at the present time are:

(1) The field rms distortion value, using the present theodolite system and Type B or Type (F − D + A) for the 64-m-diam antenna, should be within ±0.08 mm (0.003 in.) of the true value.

(2) For a practical answer, the Type B analysis method could be used for the present theodolite system. This is the method used to report the field rms distortion described in Ref. 4.

(3) The Type C method requires very precise theodolite measurements, a condition marginally accomplished at the present time.

(4) There is a definite need to improve the accuracy of the field measurement method, if the method is used for larger antennas.

(5) The NASTRAN computer analysis, used for the structural model plates and rigid jointed bars in the tie truss and the rectangular girder, definitely improves the fit between the analytic results and field measurements.

Table 2. 64-m-diam antenna reflector structure rms distortions after best fit (focal length change included)[a]

Type	RMS analysis method	Horizon look rms value, mm (in.)	Zenith look rms value, mm (in.)
	Tricone cassegrain system		
A	[b]Standard field measurement	0.91 (0.036)	1.45 (0.057)
B	[b]Assumed normal direction field measurement	0.97 (0.038)	1.57 (0.062)
C	[b]Field reads + analytical directions (field subroutine)	1.09 (0.043)	1.63 (0.064)
D	Theoretical field reads (ANAFLD subroutine)	0.94 (0.037)	1.40 (0.055)
F	Latest NASTRAN analysis ½ reflector model + some rigid joints	1.01 (0.040)	1.52 (0.060)
	Monocone cassegrain system		
A′	[b]Standard field measurement	0.81 (0.032)	1.45 (0.057)
B′	[b]Assumed normal direction field measurement	0.86 (0.034)	1.60 (0.063)
E′	STAIR analysis ¼ reflector model + pin joints	1.01 (0.040)	1.90 (0.075)
F′	Latest NASTRAN analysis ½ reflector model + some rigid joints	0.94 (0.037)	1.40 (0.055)

[a]Surface panels were set at 45-deg elevatio...
[b]Horizon field measurements were made at 6-deg elevation.

References

1. Katow, M. S., and Schmele, L. W., "Antenna Structures: Evaluation Techniques of Reflector Distortions," in *Supporting Research and Advanced Development*, Space Programs Summary 37-40, Vol. IV, pp. 176–184. Jet Propulsion Laboratory, Pasadena, Calif., Aug. 31, 1966.

2. Levy, R., "A Theoretical Consideration in the Comparison of Measured and Computed Reflector Distortions," in *The Deep Space Network*, Space Programs Summary 37-61, Vol. II, pp. 102–107. Jet Propulsion Laboratory, Pasadena, Calif., Jan. 31, 1970.

3. Bathker, D. A., *Radio Frequency Performance of a 210-Ft. Ground Antenna: X-Band*, Technical Report 32-1417. Jet Propulsion Laboratory, Pasadena, Calif., Dec. 15, 1969.

4. Katow, M. S., "Techniques Used to Evaluate the Performance of the NASA/JPL 210-Foot Reflector Structure Under Environmental Loads," in *Structures Technology for Large Radio and Radar Telescope Systems*. Edited by J. W. Mar and H. Liebowitz. The M.I.T. Press, Cambridge, Mass., 1969.

Appendix A

Coordinate Transformation of the Deflection Vectors to the Theodolite's Measuring Plane

With the measuring plane restricted to rotation θ only about axis 0Z (Fig. 2), only X and Y components of deflection vectors are transformed.

Based on the basic coordinate system,

$$\left.\begin{aligned} \mathbf{U} &= r\cos\phi \\ \mathbf{V} &= r\sin\phi \end{aligned}\right\} \qquad \text{(A-1)}$$

where

$$r = (\mathbf{U}^2 + \mathbf{V}^2)^{1/2}$$

Transformed to the measuring plane,

$$\left.\begin{aligned} \mathbf{U}'' &= r\cos(\phi - \theta) = r\cos\phi\cos\theta + r\sin\phi\sin\theta \\ \mathbf{V}'' &= r\sin(\phi - \theta) = r\sin\phi\cos\theta - r\cos\phi\sin\theta \end{aligned}\right\} \qquad \text{(A-2)}$$

Substituting Eq. (A-1) into Eq. (A-2) results in

$$\left.\begin{aligned} \mathbf{U}'' &= \mathbf{U}\cos\theta + \mathbf{V}\sin\theta \\ \mathbf{V}'' &= \mathbf{V}\cos\theta - \mathbf{U}\sin\theta \\ \mathbf{W}' &= \mathbf{W} \end{aligned}\right\} \qquad \text{(A-3)}$$

Also, for target point Q, if Q has components (X_Q, Y_Q, Z_θ),

$$X'_Q = (X_Q^2 + Y_\theta^2)^{1/2}$$

$$Y'_Q = 0$$

$$Z'_\theta = Z\psi$$

$$\theta = \tan^{-1}\frac{Y}{X}$$

Also, in this coordinate system, the vector $\mathbf{QT}/\|\mathbf{QT}\|$ has components (F'_X, F'_Y, F'_Z), where

$$F'_X = \sin\psi$$

$$F'_Y = 0$$

$$F'_Z = \cos\psi$$

Appendix B

Resolution of the Field Measurement Vectors with the Analytically Computed Directions

The magnitude of the theoretical deflection vector **QP′** in Fig. 3 is computed as follows.

If the direction vectors of **QP′** are (**U′**, **W′**), then from

$$\mathbf{S} \doteq [(\mathbf{U}')^2 + (\mathbf{W}')^2]^{1/2}$$

vector

$$\mathbf{QP}' = \|\mathbf{QP}\| \left(\frac{\mathbf{U}'}{\mathbf{S}}, \frac{\mathbf{W}'}{\mathbf{S}}\right) = \|\mathbf{QP}\| (\mathbf{U}'', \mathbf{W}'')$$

where **U″** and **W″** are unit vector components of **QP′**. If the unit vector of **QT** has components (F'_X, F'_Z), the circle product of **QP′** and the unit vector of **QT** equal **QT** when angle **QTP′** = 90 deg (because we assume that the two lines of sight are parallel) or

$$(F'_X, F'_Z) \cdot \|\mathbf{QP}\| (\mathbf{U}'', \mathbf{W}'') = \|\mathbf{QT}\|$$

Transposing,

$$\|\mathbf{QP}\| = \frac{\|\mathbf{QT}\|}{F'_X \mathbf{U}'' + F'_Z \mathbf{W}''} \tag{B-1}$$

To then compute for the magnitude of the normal error **QN**, when angle QNP = 90 deg:

$$\|\mathbf{QN}\| = \text{projection of } \mathbf{QP}' \text{ onto the unit normal}$$

When N_X and N_Z are unit vector components of the normal,

$$\|\mathbf{QN}\| = (N_X, N_Z) \cdot \|\mathbf{QP}\| (\mathbf{U}'', \mathbf{W}'') \tag{B-2}$$

Substituting Eq. (B-1) into Eq. (B-2),

$$\|\mathbf{QN}\| = \frac{\|\mathbf{QT}\| (N_X \mathbf{U}'' + N_Z \mathbf{W}'')}{(F'_X \mathbf{U}'' + F'_Z \mathbf{W}'')}$$

To establish compatibility with the rms analysis, the normal distortion $\|\mathbf{QN}\|$ is converted to a ΔZ by

$$\mathbf{QL} = \frac{\|\mathbf{QN}\|}{\cos\psi} = \frac{|\mathbf{QN}\|}{N_Z}$$

Appendix C

Resolution in the Measuring Plane to Simulate Field Measurements

In Fig. 3, the circle product of the two vectors

$$\mathbf{QT} \text{ and } \mathbf{QP}' = \|\mathbf{QT}\| \times \|\mathbf{QP}\| \times \cos\theta$$

If vector $\mathbf{QT}'$ is a unit vector in the direction of $\mathbf{QT}$, then

$$\|\mathbf{QT}\| = 1 \times \|\mathbf{QP}\| \cos\theta$$

which is equal to

$$\|\mathbf{Q}\| = \mathbf{U}'\,\mathbf{U}'' + \mathbf{W}\,\mathbf{W}'$$

where

$$\mathbf{U}'' = -1 \times \sin\psi$$

$$\mathbf{W}' = 1 \times \cos\psi$$